JMEPEG (2012) 21:920–926
DOI: 10.1007/s11665-011-9981-5

1059-9495/$19.00

Effect of Post-Weld Annealing Treatment on Plastic Deformation of 2024 Friction-Stir-Welded Joints

S.J. Yuan, Z.L. Hu, X.S. Wang, G. Liu, and H.J. Liu

(Submitted January 20, 2011; in revised form March 30, 2011)

Post-weld annealing treatment (PWAT) process was developed to improve the plasticity of friction-stir-welded 2024 aluminum alloy. The effect of the PWAT on plastic deformation behavior and microstructure of the joints were studied using tensile test, the ASAME® automatic strain measuring system, and the electron backscattered diffraction (EBSD). It is found that the elongation of the as-welded joint can be improved by PWAT and increases with the decreasing PWAT temperature. The maximum elongation of the PWAT joints can reach up to 160% of that of the as-welded joint, and the joints exhibit no decrease in the tensile strength. The deformation inhomogeneity of the as-welded joint is significantly improved by large plastic strain occurring in the thermo-mechanically affected zone (TMAZ) when the PWAT temperature is lower than 250°. As the PWAT temperature increases, the deformation in the weld nugget is found to be more beneficial than that in the TMAZ for improving the plasticity of the joint. The high plasticity of the joint is attributed to the presence of the fine-equiaxed grains in the weld nugget during PWAT.

Keywords aluminum, heat treating, mechanical testing, welding

1. Introduction

Aluminum alloys have been widely applied as one of lightweight materials for automotives and aircrafts to help in meeting the demand of fuel saving. Aluminum alloy welds have been attracting greater interest especially in the manufacture of lightweight structures (Ref 1-4). The U.S. Department of Energy (DOE), the Pacific Northwest National Laboratory (PNNL), and the U.S. Council for Automotive Research (USCAR) investigated the potential application of seam-welded tubes and tailor-welded blanks of aluminum alloy in automotive industry. The deformation of the weld material and the formability were found to be the important factors of consideration during the fabrication of automotive parts (Ref 5). When aluminum alloy welds are used in automotive and aircraft industry, the most difficult challenge to be met is that they must exhibit adequate plasticity similar to that of the base material (BM) to shape the required complex geometries (Ref 6). However, conventional fusion welding methods often lead to significant strength deterioration and low plasticity in the joint because of a dentritic structure formed in the fusion zone (Ref 7).

Friction-stir welding (FSW), as a solid-state metal joining technique, is well suited for joining aluminum alloys and shows better mechanical properties, as there is far lower heat input during this process than when compared with conventional welding methods (Ref 8, 9). Many studies based on experiments and simulations (Ref 10-14) have been focused mainly to understand the FSW process itself, especially the effect of process parameters on the quality of welding, such as tool geometry, rotation speed, and base materials. Studies on improving the plasticity of FSW aluminum alloys are rare except for the recent few that investigated the formability of FSW joints (Ref 4-6, 15, 16). Garware et al. (Ref 4) studied the tensile behavior of FSW joints in a tailor-welded blank of aluminum alloy 5754. The results showed that the elongation of the joints were only half of that of the BM. Merklein et al. (Ref 6) investigated the achievable hardness of FSW seams as an indicator of the formability of 6016, and showed that there was a huge increase of the hardness in the weld seam caused by the deep-drawing process. Miles ea al. (Ref 15) examined the formability of FSW 6022-T4 sheets and found that the joints retained about 43% of the BM elongation with the weld, transverse to the tensile axis. Buffa et al. (Ref 16) reported that the welding parameters of FSW Al 7075-T6-tailored blanks had to be carefully designed to obtain high-quality joints. The above cited studies have shown that the plasticity of FSW joints is low, and the application of FSW welds in automotive and aircraft industry has been quite limited.

To improve the mechanical properties of the joints, one option is to adopt the fully post-weld heat treatment (PWHT) of the welded components. The PWHT consisted of solution heat treatment and precipitation or aging treatment, aiming to recover the loss of tensile strength in the weld nugget (WN) (Ref 17-22). A few studies on the PWHT of FSW aluminum alloys, such as 7475 (Ref 22), 7449 (Ref 18), 6061-O (Ref 21), 6063-T5 (Ref 20), 2219-O (Ref 17), and 2024-T4 (Ref 19) have shown that the strength of FSW joints can be improved. However, the fine-equiaxed grains in the WN are not stable during the process and result in a sharp decrease in the elongation (about 40-77%) compared to those of the BM. Moreover, several authors have investigated the effect of

S.J. Yuan, Z.L. Hu, X.S. Wang, G. Liu, and **H.J. Liu**, National Key Laboratory of Advanced Welding Production Technology, Harbin Institute of Technology, Harbin 150001, People's Republic of China. Contact e-mail: hitxswang@hit.edu.cn.

friction-stir processing (FSP) on superplastic deformation behaviors of a few aluminum alloys (Ref 23-25). It is reported that the fine-grained aluminum alloys prepared by FSP would exhibit superplastic behavior at a very slow strain rate combined with high temperature. However, from an industrial point of view, such approach is often too costly, and treated as not feasible.

Normally, aluminum alloy blanks used for joining are applied in T4 or T6 treatments. However, if the base material (BM) is in O condition, then the post-weld forming operation can be performed much more easily for realizing the high plasticity (Ref 21, 26). Furthermore, the post-weld solution and the aging heat treatment can later restore the mechanical properties of the joints successfully (Ref 17-22). In this study, an attempt is made to improve the plasticity of FSW 2024-O aluminum alloy by post-weld annealing treatment (PWAT) process. The emphasis is placed on investigating the effect of PWAT on plastic deformation behavior and microstructure of FSW joints.

2. Experimental Procedures

2.1 Material and Friction-Stir Welding Conditions

A few 5-mm-thick rolled plates of 2024-O aluminum alloy were friction-stir welded vertical to the rolling direction employing a rotational speed of 600 rpm and a travel speed of 300 mm/min. The threaded pin of the tool had a diameter of 5 mm and a length of 4.9 mm. Shoulder was selected to be 14 mm in diameter, and the tilt angle was set equal to 3°.

2.2 Post-Weld Annealing Treatments

After welding, the plates were cut into two parts, one part for the PWAT and the other for as-welded examinations. The PWAT included annealing at different temperatures from 250° to 450°, in steps of 50° for 2 h, followed by cooling in the furnace to 200°.

2.3 Metallography

Following the FSW and PWAT, the specimens were cut perpendicular to the welding direction. The orientation-imaging microscope (OIM) was attached to an S-570/HITACHI-4700 scanning electron microscope operating at 25 kV. The OIM images were used to evaluate grain size distribution with step size of 1 μm. The fraction of special microstructure, such as the deformed/recrystallized microstructure, was analyzed using the Channel 5 software from HKL Technology, Inc.

2.4 Mechanical Tests

The Vickers micro-hardness test was carried out across the joint at depths of 1.5, 2.5, and 3.5 mm from the upper surface with a distance between neighboring measured points of 2 mm under a load of 100 g for 10 s. The tensile tests were performed at a crosshead speed of 2 mm/min using an Instron-1186 testing machine. An axial extensometer with 25-mm gage length was attached to the test specimens at the gauge section. The strain analysis of each specimen was made by the ASAME® automatic strain measuring system, and the tensile properties of the joints were evaluated using the three tensile specimens cut out from the same joint.

3. Results and Discussion

3.1 Microstructures

The upper-surface appearance of the FSW plate and the cross section of the weld are indicated in Fig. 1(a) and (b), respectively. The FSW joint shows good weld quality with no wormhole and kissing-bond defects. A basin-shaped nugget that widens near the upper surface can be observed in Fig. 1(b). This is because the upper surface experiences extreme deformation and frictional heating because of contact with a cylindrical-tool shoulder during FSW (Ref 27).

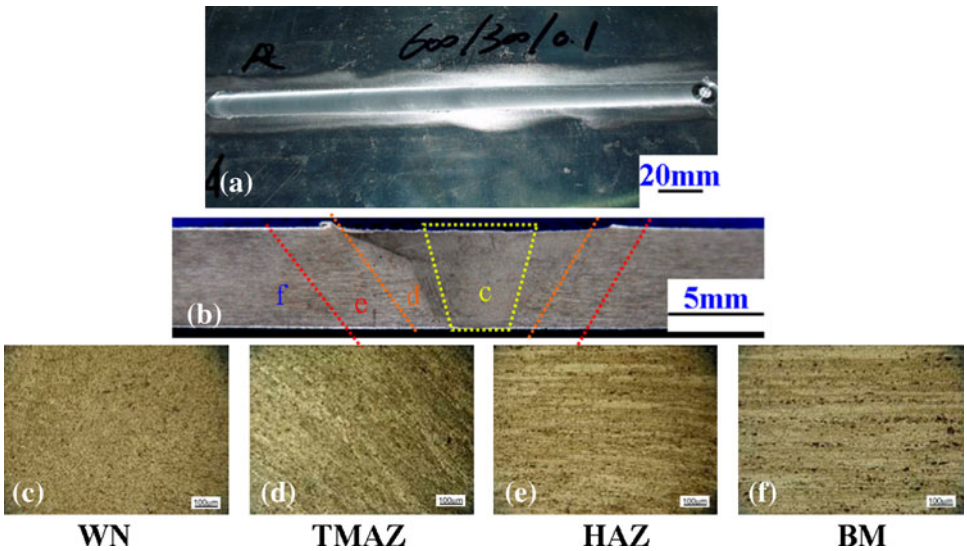

Fig. 1 (a) Upper surface appearance of FSW joint, (b) cross section perpendicular to the welding direction, (c) microstructure of WN, (d) microstructure of TMAZ, (e) microstructure of HAZ, and (f) microstructure of BM

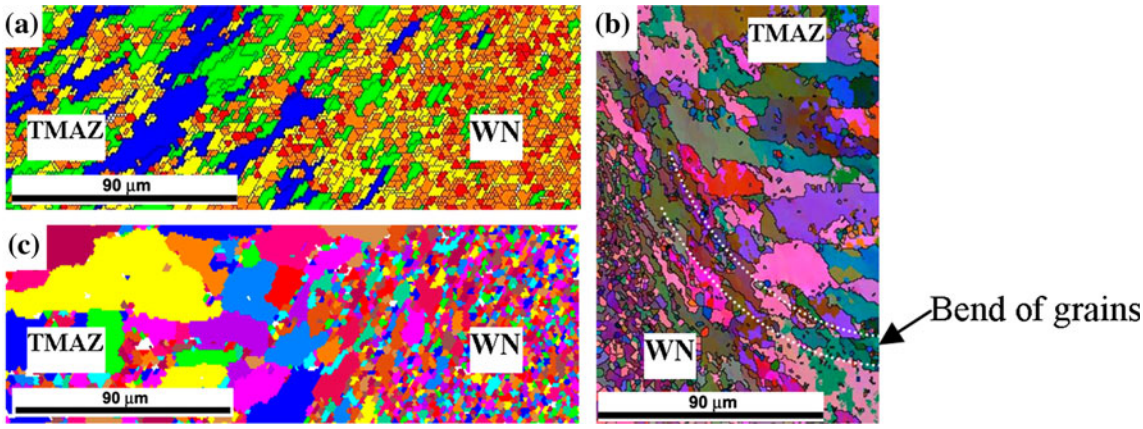

Fig. 2 OIM images showing the microstructure of the FSW joints: (a) as-welded, (b) 300°, and (c) 450°

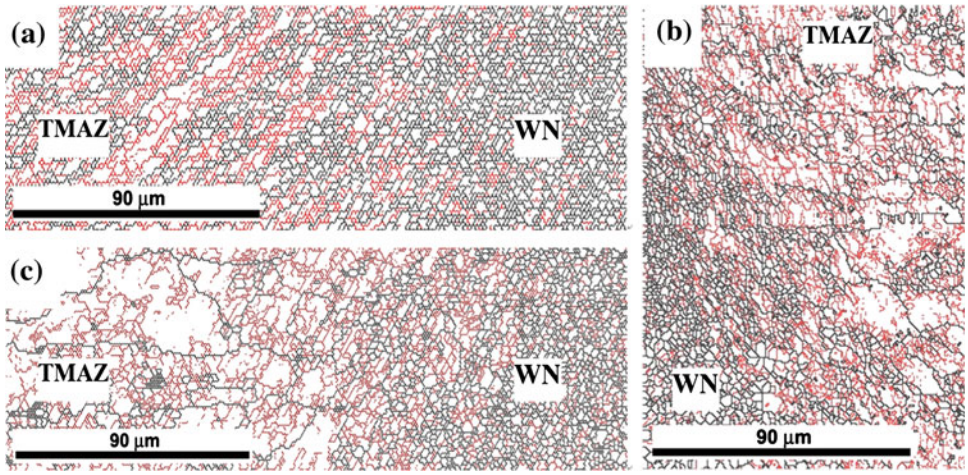

Fig. 3 EBSD images showing the grain boundary of the FSW joints: (a) as-welded, (b) 300°, and (c) 450°

A friction-stir weld is conventionally divided into four regions, i.e., WN, thermo-mechanically affected zone (TMAZ), heat-affected zone (HAZ), and BM, as shown in Fig. 1. The WN of the as-welded joint consists of very fine-equiaxed grains with average grain size of 1.7 μm (Fig. 1c). The microstructural changes occur immediately adjacent to the WN. The initial grains in the TMAZ are rotated and elongated in an upward flowing pattern around the WN (Fig. 1d). Beyond the TMAZ, there is a HAZ. In this zone, the plastic deformation is absent or insufficient to modify the initial grain structure (Fig. 1e). This zone has been subjected to only thermal alterations, and it retains the same grain structure as the BM (Fig. 1f).

Figure 2 shows the OIM images of the FSW joints in the transition zone from the WN to the TMAZ. The average grain sizes are 1.8 and 2.0 μm in the WN of 300° and 450° PWAT joint, respectively (Fig. 2b, c). It indicates that the fine-equiaxed microstructure in the WN is stable during PWAT, even when the PWAT temperature is increased up to 450 °C. The vast majority of the grain boundaries in the WN have a high angle ($>15°$), regardless of as-welded joints or PWAT joints (Fig. 3). It is proven that the full dynamic recrystallization occurs in the WN during FSW. As a result, fine dynamically recrystallized and equiaxed grains in the WN are stable during PWAT.

The TMAZ lies outside the WN and is still distinguishable from the WN after the PWAT. The majority of rotated and elongated grains in the TMAZ of the joint have been equiaxed after PWAT at 300°, and only few of the grains in the TMAZ are slightly rotated and elongated (Fig. 2b). Furthermore, nearly all the grains in the TMAZ of the joint become equiaxed and coarse after PWAT at 450° (Fig. 2c). The density of the small-angle grain boundary ($<15°$) in the TMAZ decreases and the vast majority of the grain boundaries in the TMAZ have a high angle ($>15°$) after the PWAT (Fig. 3b, c). It is suggested that recrystallization occurs in the TMAZ during the PWAT. As a result, the elongated grains in the TMAZ of the joints will coarsen when the PWAT temperature is higher than 300°.

Figure 4 shows the fraction of special microstructure in the TMAZ of the joints. The variations in the fraction of special microstructure can possibly explain the reason for grain coarsening in the TMAZ. The grains in the TMAZ of the as-welded joint, experiencing both temperature and deformation during FSW (Ref 7-10), usually contain a high density of sub-boundaries as shown in Fig. 4. This substructure merges into the subgrains, which are apt to grow into big equiaxed grains during PWAT (Ref 8, 9). The phenomenon is more pronounced as the PWAT temperature increases. Finally, the

most deformed microstructure in the TMAZ is changing into the recrystallization microstructure after the PWAT at 450°.

3.2 Microhardness

Figure 5 shows the typical microhardness across the joints in different thicknesses. The top of the joints are significantly harder than the bottom, regardless of as-welded or PWAT joints. It is mainly because that the upper surface experiences extreme deformation and frictional heating during FSW, thereby resulting in generation of more fine recrystallized grains than that of the bottom. According to the Hall-Petch relationship, the WN has a much higher hardness than the base materials because of its fine grains. After PWAT, the gap of the micro-hardness, between the top and the bottom in the weld zone, is not so obvious and decreases with the increasing PWAT temperature. The micro-hardness in the WN is higher than that of BM when the PWAT temperature is low, which is due to the retention of a large amount of deformation microstructure and fine grains in the weld during PWAT at the low temperature. As the PWAT temperature increases, micro-hardness in the WN decreases. However, it is still slightly higher than that of the BM for the reservation of the fine grains in the weld during PWAT.

3.3 Tensile Properties and Fracture Surfaces

Figure 6 displays the tensile properties of the joints and the BM. The elongation, yield strength, and tensile strength of BM, are 22.2%, 88 MPa, and 207 MPa, respectively. The as-welded joint possesses the same tensile strength as the BM, but the elongation of the joint is 12.5%, which signifies a 44% reduction compared with that of the BM. The PWAT joints exhibit significantly different mechanical properties. The elongations of the 450°, 400°, 350°, and 300° PWAT joints are 10.7%, 14.7%, 18.9%, and 20.2%, respectively. It indicates that the elongation of the PWAT joints increase with decreasing PWAT temperature. In contrast, the tensile strength of the PWAT joints changes little with temperature. All PWAT joints show nearly the same tensile strength as those of the BM. The results suggest that the plasticity of the as-welded joint can be improved by PWAT effectively with no loss of tensile strength.

Figure 7 shows the fracture locations of the joints before and after PWAT. The as-welded joint is fractured at the BM on the advancing side (Fig. 7a). It is because the WN is composed of the recrystallized fine-equiaxed grains (Fig. 2a) for experiencing intense plastic deformation and frictional heating during FSW (Ref 7, 19, 27). The joint is strengthened by FSW process, and thus fails at the BM. After the PWAT, the joints are fractured at the BM when the PWAT temperature is lower than 300° (Fig. 7b). However, the joints are fractured at the interface between the WN and TMAZ on the advancing side as the PWAT temperature increases (Fig. 7c). The cross-sectional details of the fracture location of the 450° PWAT joints are shown in Fig. 7(d). It indicates that the fracture locations of the joints change with the PWAT temperature. This can be explained by the inner structure of the joints. The joint consists of both

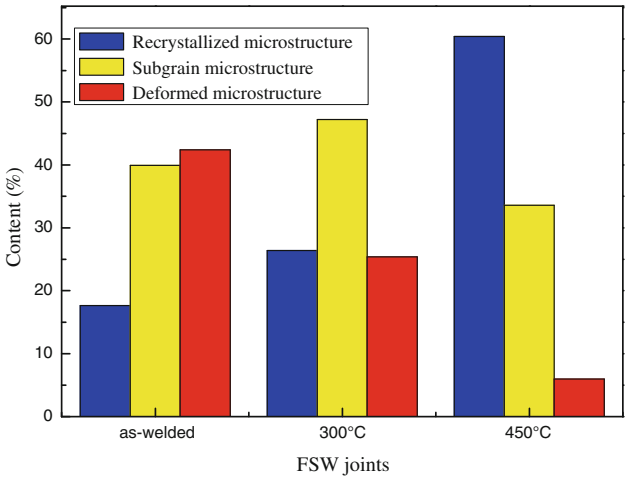

Fig. 4 Fraction of the special microstructure in the TMAZ of FSW joints

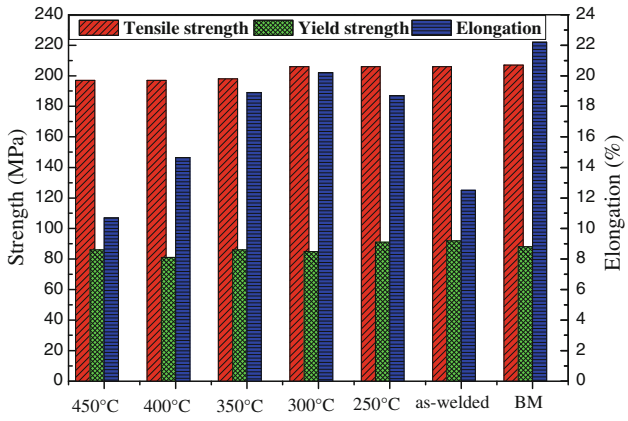

Fig. 6 Comparison of the tensile properties of the BM, the as-welded, and PWAT joints

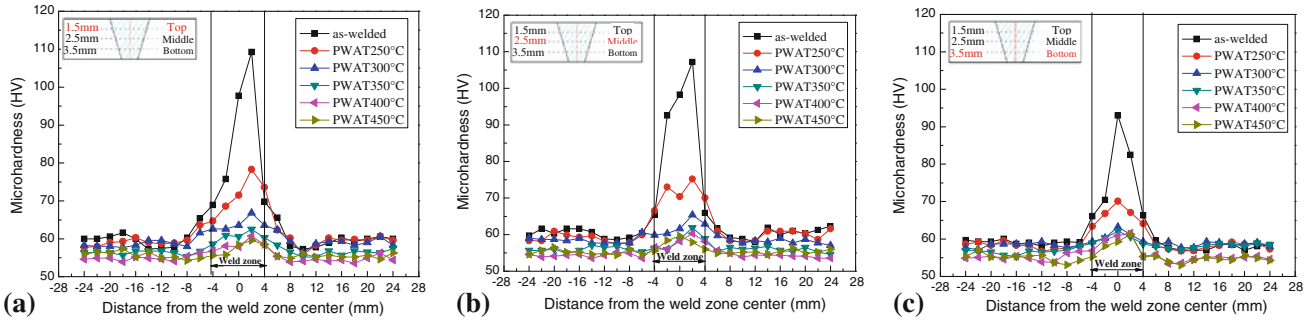

Fig. 5 Micro-hardness across the joint at depths of 1.5, 2.5, and 3.5 mm from the upper surface. (a) Micro-hardness in the top of the cross sections, (b) micro-hardness in the middle of the cross sections, and (c) micro-hardness in the bottom of the cross sections

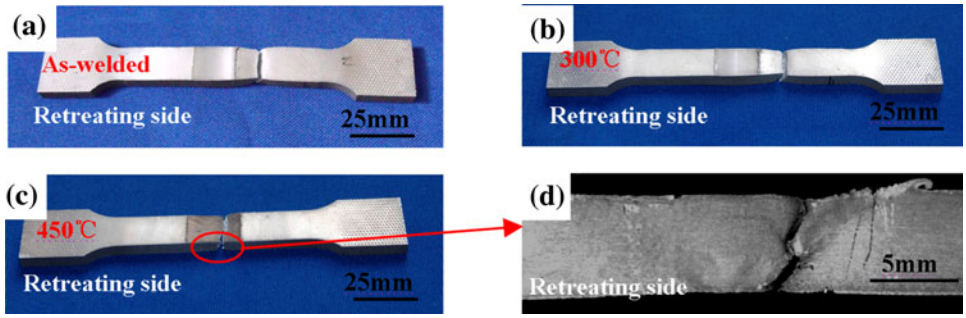

Fig. 7 The fracture of FSW joints: (a) as-welded, (b) 300°, (c) 450°, and (d) macro fracture cross section of 450° PWAT joint

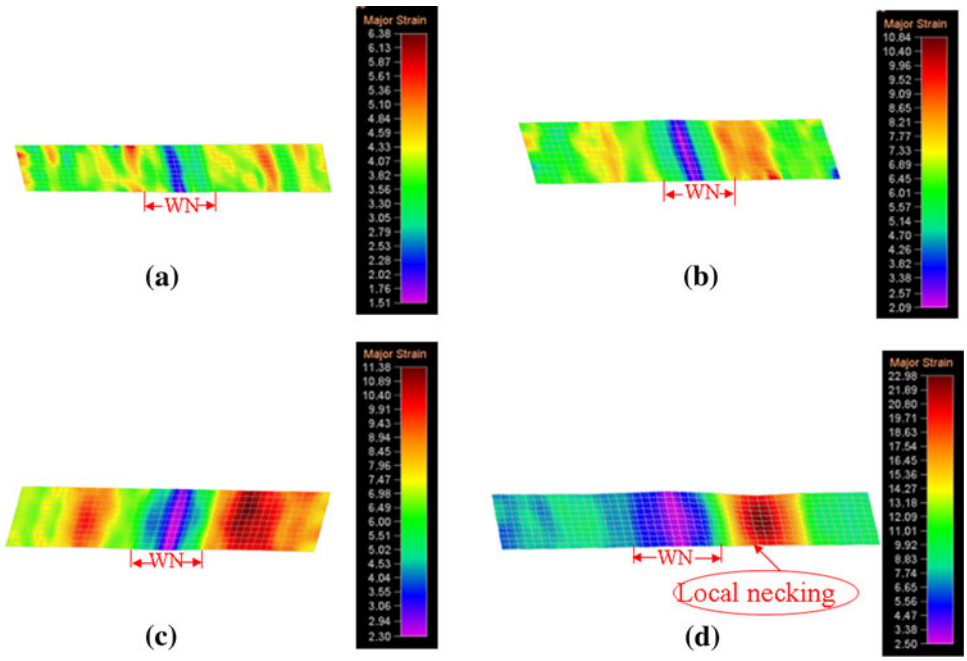

Fig. 8 Evolution of the plastic strain distribution in the gauge section of as-welded joint. Plastic strain of (a) 2%, (b) 5%, (c) 7%, and (d) 10%

fine-equiaxed grains and the highly deformed microstructure when the PWAT temperature is low (Fig. 2b). Thus, the joint shows a higher strength than that of the BM and leads to fracture at the BM. In addition, nearly all the grains in the TMAZ of the joints become equiaxed and coarse as the PWAT temperature increases (Fig. 2c). The interface between the WN and the TMAZ is more clearly visible and becomes a weaker region, resulting in the fracture along the interface, as seen in Fig. 7(d).

3.4 Plastic Deformation of Joints

Figure 8 shows the evolution of the strain distribution in the as-welded joint of the four samples with global plastic strains of 2%, 5%, 7%, and 10%, respectively. The evolution of the plastic strain distribution shows that plastic strain concentrates in the BM (in the region of 10 mm), and is the lowest in the WN (in the region of 8 mm) at very early stage, as seen in Fig. 8(a) and (b). Deformation on both sides of the WN stays roughly symmetrical until a global plastic strain of 7%, after which strain localization occurs in the BM on advancing side. Local strain larger than 11.4% is observed. Simultaneously, the local strain in the WN is observed to be only 2.3% (Fig. 8c). When the global plastic deformation of the joint reaches 10%, local necking can be observed with a local strain of 23%, and a fracture tends to develop. However, the local strain in the WN is only 2.5-3.3% at this stage (Fig. 8d). It shows that the regional deformation of the as-welded joint is highly inhomogeneous. This is attributed to the grain refinement in the WN by FSW process resulting in a comparatively high deformation resistance in the weld during tensile test. It can be concluded that the highly inhomogeneous deformation throughout the joint, caused by heterogeneous microstructure, is the reason for the 44% decrease in elongation of the as-welded joint compared with that of the BM.

Figure 9 shows the strain distribution in the gauge section of the FSW joints. The stain in the WN of the 250° PWAT joint is low, which is the same as that of the as-welded joint. Nevertheless, the strain in the TMAZ of the joint is very high, causing a large deformation in the adjacent BM. The elongation of the joint increases compared to that of the as-welded joint. It can be concluded that the increase in the elongation of the PWAT joint mainly depends on the deformation in the TMAZ when the PWAT temperature is lower than 250°. It is mainly because the recovery is apt to occur in the TMAZ of the joint during

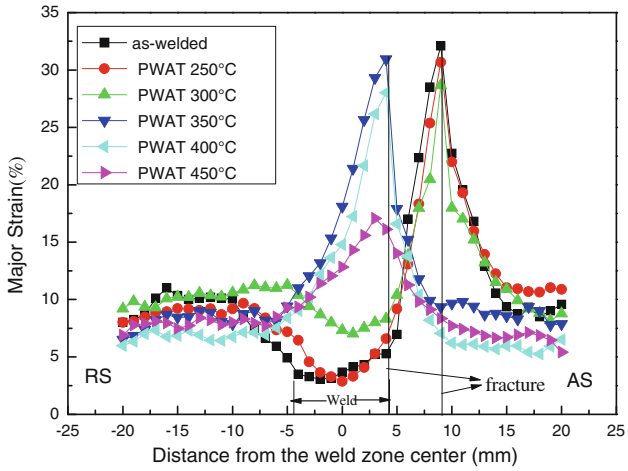

Fig. 9 Plastic strain distribution in the gauge section of FSW joints

the PWAT at low temperature for containing the highly deformed microstructure, leading to the softening in the TMAZ.

As shown in Fig. 9, the strain map of the 300° PWAT joint reveals relatively homogeneous deformation. The average strains in the WN and BM are about 8 and 12%, respectively. It indicates that the deformation inhomogeneity of the joint has been improved by both the weld and the BM showing large strain. Moreover, the deformation in the WN of the joint increases with the increasing PWAT temperature and the local strain in the WN exceeds 30% except 450° PWAT joint. The deformation inhomogeneity in the joint is improved, and the elongation of the PWAT joint increases. It suggests that the plasticity of the PWAT joint mainly depends on the deformation in the WN when the PWAT temperature is higher than 300°. This is mainly because the WN of the PWAT joints show better plasticity than that of the TMAZ. The WN of the joint is composed of the fine-equiaxed grains, which are retained during PWAT, while TMAZ is constituted by coarse-equiaxed grains. Therefore, the deformation in the WN is larger and plays a greater role on improving the elongation of the PWAT joint. Moreover, the elongation of the 450 °C PWAT joint is slightly lower than that of the as-welded joint. It can be attributed to the low fracture toughness of the joint for grain coarsening occurring in the TMAZ after PWAT at 450°.

4. Conclusions

(1) The optimum PWAT process parameters are annealing at 300° for 2 h, and then cooling in the furnace to 200°. The elongation of the 300° PWAT joint can reach up to 160% of that of the as-welded joints. The plasticity of the FSW joint can be significantly improved by the PWAT process.

(2) The increase in the elongation of the PWAT joint mainly depends on the deformation in the TMAZ, when the PWAT temperature is lower than 250°. As the PWAT temperature increases, deformation in the WN is found to be more beneficial than that in the TMAZ, with improvement in the plasticity of the joint

(3) The top of the joints are significantly harder than the bottom regardless of as-welded joints or PWAT joints. The gap of the microhardness, between the top and the bottom in the weld zone, is not so obvious and decreases with increasing PWAT temperature.

(4) The joints fail at the BM after the PWAT at 300°. As the PWAT temperature increases, the joints are fractured at the interface between the WN and the TMAZ on the advancing side.

(5) The fine-equiaxed grains are retained in the WN even the PWAT temperature is up to 450°. However, the grains in the TMAZ become coarsened with increasing PWAT temperature.

References

1. K. Hariharan, G. Balachandran, and M. Sathya Prasad, Application of Cost-Effective Stainless Steel for Automotive Components, *Mater. Manuf. Process.*, 2009, **24**, p 1442–1452
2. S.J. Yuan, C. Han, and X.S. Wang, Hydroforming of Automotive Structural Components with Rectangular-Sections, *Int. J. Mach. Tool Manuf.*, 2006, **46**, p 1201–1206
3. R.M. Natal Jorge, R.A.F. Valente, A.P. Roque, M.P.L. Parente, and A.A. Fernandes, Numerical Simulation of Hydroforming Process Involving a Tubular Blank with Dissimilar Thickness, *Mater. Manuf. Process.*, 2007, **22**, p 286–291
4. M. Garware, G.T. Kridli, and P.K. Mallick, Tensile and Fatigue Behavior of Friction-Stir Welded Tailor-Welded Blank of Aluminum Alloy 5754, *JMEPEG*, 2010, **19**, p 1161–1171
5. R.W. Davies, J.A. Carpenter, P.S. Sklad, and E.V. Stephens, Forming Limits of Weld Material in Aluminum Alloys and High-Strength Steels, *United States Automotive Materials Partnership AMD Offsite Annual Review Meeting*, Detroit, 2005
6. M. Merklein, M. Wieland, and D. Staud, Friction Stir Welds Made out of Precipitation Hardenable Aluminum Alloys-Experimental Investigations of Formability Potential, *Int. J. Mater. Forming*, 2009, **2**, p 323–326
7. C. Genevois, A. Deschamps, A. Denquin, and B. Doisneau-cottignies, Quantitative Investigation of Precipitation and Mechanical Behaviour for AA2024 Friction Stir Welds, *Acta Mater.*, 2005, **53**, p 2447–2458
8. R. Nandan, T. DebRoy, and H.K.D.H. Bhadeshia, Recent Advances in Friction-Stir Welding-Process, Weldment Structure and Properties, *Prog. Mater. Sci.*, 2008, **53**, p 980–1023
9. R.S. Mishra and Z.Y. Ma, Friction Stir Welding and Processing, *Mater. Sci. Eng. Rep.*, 2005, **50**, p 1–78
10. J.D. Robson, N. Kamp, and A. Sullivan, Microstructural Modelling for Friction Stir Welding of Aluminium Alloys, *Mater. Manuf. Process.*, 2007, **22**, p 450–456
11. T.S. Srivatsan, S. Vasudevan, L. Park, and R.J. Lederich, The High Cycle Fatigue and Fracture Behavior of Friction Stir Welded Aluminum Alloy 2024, *KEM*, 2008, **378–379**, p 175–206
12. K. Weon-kyong, G. Byeong-choon, and W. Si-tae, Optimal Design of Friction Stir Welding Process to Improve Tensile Force of the Joint of A6005 Extrusion, *Mater. Manuf. Process.*, 2010, **25**, p 637–643
13. T.S. Srivatsan, S. Vasudevan, and L. Park, The Tensile Deformation and Fracture Behavior of Friction Stir Welded Aluminum Alloy 2024, *Mater. Sci. Eng. A*, 2007, **466**, p 235–245
14. K. Kumar, S.V. Kailas, and T.S. Srivatsan, Influence of Tool Geometry in Friction Stir Welding, *Mater. Manuf. Process.*, 2008, **23**, p 188–194
15. M.P. Miles, B.J. Decker, and T.W. Nelson, Formability and Strength of Friction-Stir-Welded Aluminum Sheets, *Met. Mater. Trans. A*, 2004, **35A**, p 3461–3468
16. G. Buffa, L. Fratini, J. Hua, and R. Shivpuri, Friction Stir Welding of Tailored Blanks: Investigation on Process Feasibility, *CIRP Ann.*, 2006, **55**, p 279–282
17. Y.C. Chen, H.J. Liu, and J.C. Feng, Effect of Post-Weld Heat Treatment on the Mechanical Properties of 2219-O Friction Stir Welded Joints, *J. Mater. Sci. Lett.*, 2006, **41**, p 297–299
18. A. Sullivan and J.D. Robson, Microstructural Properties of Friction Stir Welded and Post-Weld Heat-Treated 7449 Aluminium Alloy Thick Plate, *Mater. Sci. Eng. A*, 2008, **478**, p 351–360
19. H. Aydın, A. Bayram, and I. Durgun, The Effect of Post-Weld Heat Treatment on the Mechanical Properties of 2024-T4 Friction Stir-Welded Joints, *Mater. Des.*, 2010, **31**, p 2568–2577

20. Y.S. Sato, S.H.C. Park, and H. Kokawa, Microstructural Factors Governing Hardness in Friction-Stir Welds of Solid-Solution-Hardened Al Alloys, *Met. Mater. Trans. A*, 2001, **32A**, p 3033–3042
21. K.N. Krishnan, The Effect of Post Weld Heat Treatment on the Properties of 6061 Friction Stir Welded Joints, *J. Mater. Sci.*, 2002, **37**, p 473–480
22. I. Charit, R.S. Mishra, and M.W. Mahoney, Multi-Sheet Structures in 7475 Aluminum by Friction Stir Welding in Concert with Post-Weld Superplastic Forming, *Scripta Mater.*, 2002, **47**, p 631–636
23. Z.Y. Ma, R.S. Mishra, and M.W. Mahoney, Friction Stir Processing for Microstructural Modifications of an Aluminum Casting, *Acta Mater.*, 2002, **50**, p 2219–2230
24. H.G. Salem, A. Reynolds, and J. Lyons, Microstructure and Retention of Superplasticity of Friction Stir Welded Superplastic 2095 Sheets, *Scripta Mater.*, 2001, **45**, p 337–342
25. H.G. Salem, A.P. Reynolds, and J.S. Lyons, Structural Evolution and Superplastic Formability of Friction Stir Welded AA 2095 Sheets, *JMEPEG*, 2004, **13**, p 24–31
26. J.C. Feng, Y.C. Chen, and H.J. Liu, Effects of Post-Weld Heat Treatment on Microstructure and Mechanical Properties of Friction Stir Welded Joints of 2219-O Aluminium Alloy, *Mater. Sci. Technol.*, 2006, **22**, p 86–90
27. K. Kumar, C. Kalyan, V. Kailas Satish, and T.S. Srivatsan, An Investigation of Friction during Friction Stir Welding of Metallic Materials, *Mater. Manuf. Process.*, 2009, **24**, p 438–445